

Technical report 11-043

Kalman Filter-Based Distributed Predictive Control of Large-Scale Multi-Rate Systems: Application to Power Networks*

S. Roshany-Yamchi, M. Cychowski, R. R. Negenborn,
B. De Schutter, K. Delaney, and J. Connell

To cite this work, please refer to the published version:

S. Roshany-Yamchi, M. Cychowski, R. R. Negenborn, B. De Schutter, K. Delaney, and J. Connell, "Kalman filter-based distributed predictive control of large-scale multi-rate systems: Application to power networks," *IEEE Transactions on Control Systems Technology*, vol. 21, no. 1, pp. 27–39, Jan. 2013. doi:[10.1109/TCST.2011.2172444](https://doi.org/10.1109/TCST.2011.2172444)

Delft Center for Systems and Control
Delft University of Technology
Mekelweg 2, 2628 CD Delft
The Netherlands
phone: +31-15-278.24.73 (secretary)
URL: <https://www.dcsc.tudelft.nl>

* This report can also be downloaded via <https://dpub.eu/11-043>

Kalman Filter-Based Distributed Predictive Control of Large-Scale Multi-Rate Systems: Application to Power Networks

Samira Roshany-Yamchi, *Student Member, IEEE*, Marcin Cychowski, *Member, IEEE*, Rudy R. Negenborn, Bart De Schutter, *Senior Member, IEEE*, Kieran Delaney, Joe Connell, *Member, IEEE*,

Abstract—In this paper, a novel distributed Kalman Filter (KF) algorithm along with a distributed Model Predictive Control (MPC) scheme for large-scale multi-rate systems is proposed. The decomposed multi-rate system consists of smaller subsystems with linear dynamics that are coupled via states. These subsystems are multi-rate systems in the sense that either output measurements or input updates are not available at certain sampling times. Such systems can arise, e.g., when the number of sensors is smaller than the number of variables to be controlled, or when measurements of outputs cannot be completed simultaneously because of practical limitations. The multi-rate nature gives rise to lack of information, which will cause uncertainty in the system's performance. To circumvent this problem, we propose a distributed KF-based MPC scheme, in which multiple control and estimation agents each determine actions for their own parts of the system. Via communication, the agents can in a cooperative way take one another's actions into account. The main task of the proposed distributed KF is to compensate for the information loss due to the multi-rate nature of the systems by providing optimal estimation of the missing information. A demanding two-area power network example is used to demonstrate the effectiveness of the proposed method.

Index Terms—Kalman Filter, Large-scale systems, Multi-rate systems, Model Predictive Control, Nash game.

I. INTRODUCTION

LARGE-scale distributed systems are present in many engineering application domains including process plants, road traffic networks, water and sewer networks, power distribution systems, wind farms, or wireless sensor/actuator networks [1]–[7]. The complexity of these systems is defined by their multi-agent nature and multi-actor character, their multi-level structure, their multi-objective optimization challenges, and by the adaptivity of their agents and actors to changes in their environment. For these reasons, the operation and control of large-scale systems that meet the desired economic, safety, and performance requirements is a challenging task. Strategies based on centralized control often require high computational effort and are regarded by practitioners as impractical.

Recently, considerable attention has been devoted to control and estimation problems in large-scale systems and numer-

ous distributed control [2], [8]–[12] and estimation [13]–[15] methods have been proposed. In a distributed control structure, the whole system is decomposed into a number of small subsystems. Each subsystem is controlled by a so-called *agent*, which solves its own, local control and estimation problem. State estimators can be employed to compute important states of the system that are often difficult to measure, using partly available measurement. The structure of a state estimator involves a dynamical model of the system, which is simulated in parallel to the real system using the same inputs and initial conditions as the real system. Then the simulation error, defined as the difference between the real measurements and the simulated ones, is used as feedback in the simulated model for correction. This error comes into play as the initial conditions are often not known exactly, the process is subject to disturbances, or model-plant mismatch exists. In such cases, if no feedback is used, there is no guarantee that the predictions are close or equal to the real states.

The computational effort required to implement the conventional centralized estimation algorithms (e.g. Kalman filters (KF) [16]) for large-scale systems can be prohibitive for many on-line applications. Several decentralized and distributed estimation schemes for large-scale systems have been proposed [3], [6], [17]–[19] to make the estimation problem computationally efficient.

This paper proposes a novel control and estimation method for multi-rate sampled linear systems that employs a distributed Model Predictive Control (MPC) strategy (a controller that utilizes an explicit process model as to optimize predicted future performance of the system while taking into account process operating, safety and physical constraints) in combination with a distributed KF. In multi-rate systems, either the measurements are available less frequently or the control actions are made at a lower rate. Such systems can be encountered in many industrial applications [20]–[24]. In the process industry, for instance, quality variables such as product concentration or average molecular weight distribution in a polymerization process, can be evaluated/updated at much slower rates compared to other process measurements. On the other hand, in certain biomedical applications [22] the input injection rate is inherently slower than the output measurement, e.g. in drug infusion systems, the drug injection to the patient occurs less frequently than the body symptom's measurements such as blood pressure, body temperature, etc.

Several works on predictive control and estimation for

S. Roshany-Yamchi, M. Cychowski, K. Delaney and J. Connell are with the NIMBUS Centre, Cork Institute of Technology, Ireland (e-mail: samira.roshany@cit.ie; marcin.cychowski@cit.ie; kieran.delaney@cit.ie; joe.connell@cit.ie).

R. R. Negenborn is with the Department of Marine and Transport Technology and Bart De Schutter is with the Delft Center for Systems and Control, Delft University of Technology, The Netherlands (e-mail: r.r.negenborn@tudelft.nl; b.deschutter@tudelft.nl)

multi-rate systems have appeared recently. The relevance and importance of multi-rate processes has been investigated for the centralized Generalized Predictive Control (GPC) framework in [25], [26]. In [27], the author considers a stochastic multi-rate control problem and uses a centralized generalized minimum-variance approach to solve the problem.

In [18], a distributed KF for single-rate sampled systems has been developed in which local measurements are used to estimate the relevant system states. This information is then used by a distributed MPC controller. Considering communication among local estimators and controllers provides a performance improvement in comparison with completely decentralized controllers. A distributed control system based on independent MPC and KF schemes has been developed in [19] for fault-tolerant applications. In this work, the interconnected subsystems exchange information in a cooperative way. In [28], authors presented three Moving Horizon Estimation (MHE) methods for discrete-time partitioned single-rate linear systems, in which the systems were decomposed into coupled subsystems with non-overlapping states. The presented methods have the capability of exploiting physical constraints on states and noise in the estimation process.

In [20], [29], a state-space based multi-rate MPC scheme has been developed for a centralized case in which a centralized KF is used to estimate the missing variables in inter-sampling times. We propose a new distributed MPC control strategy for large-scale systems with multi-rateness in its subsystems. This means that each of the subsystems is multi-rate in inputs and/or outputs. The multi-rate control method that we propose allows control moves to be made using state estimates from a distributed KF. A comprehensive simulation study involving a two-area power network example is used to evaluate the efficiency of the proposed method with respect to other estimation and control methodologies available in the literature.

The main contribution of this paper is the development of a generalized framework that covers both aspects of distributed control and estimation of multi-rate large-scale systems. Our focus in this paper is to develop a generic framework based on Nash game theory, for large-scale multi-rate systems with linear dynamics that are coupled via states.

This paper is organized as follows. In Section II, a distributed multi-rate model predictive control algorithm is discussed. In Section III, a distributed Kalman Filter is formulated to estimate the states in a multi-rate system. Section IV, has been devoted to applying the proposed method on a case study that is a two-area power system, followed by simulation results and analysis the performance of the proposed method in Section V. Section VI, concludes with some remarks and hints for future research.

II. DISTRIBUTED MULTI-RATE MPC

A. State-Space Model

Consider distributed MPC for systems with linear dynamics whose centralized nominal model is decomposed into m subsystems. Let t be the discrete-time index for the system under control. The following model can be written for a

distributed system with state coupling:

$$\mathbf{x}_i(t+1) = \mathbf{A}_{ii}\mathbf{x}_i(t) + \mathbf{B}_i\Delta\mathbf{u}_i(t) + \mathbf{D}_i\mathbf{v}_i(t) + \sum_{\substack{j=1 \\ j \neq i}}^m \mathbf{A}_{ij}\mathbf{x}_j(t), \quad (1)$$

$$\mathbf{y}_i(t) = \mathbf{C}_i\mathbf{x}_i(t) + \mathbf{z}_i(t), \quad (2)$$

where for each subsystem i , \mathbf{x}_i , \mathbf{u}_i , \mathbf{y}_i denote the state, input, and output variables, respectively, \mathbf{v}_i , \mathbf{z}_i are the state and measurement noise disturbances, respectively, and \mathbf{A}_{ii} , \mathbf{B}_i , \mathbf{A}_{ij} , \mathbf{D}_i and \mathbf{C}_i are the system matrices of appropriate dimensions. Also, $\Delta\mathbf{u}_i(t)$ is the increment of the input signal, defined as $\Delta\mathbf{u}_i(t) = \mathbf{u}_i(t) - \mathbf{u}_i(t-1)$. Note that the model presented in (1)–(2) is an augmented model [30]. The variable $\Delta\mathbf{u}_i(t)$ is the multi-rate input signal that is injected into the subsystems at each sampling time. As it can be seen in (1) subsystems are coupled through states only. We follow a strategy similar to [20] to implement multi-rate measurement and input calculation mechanisms for synchronous and asynchronous agents (see Fig. 1).

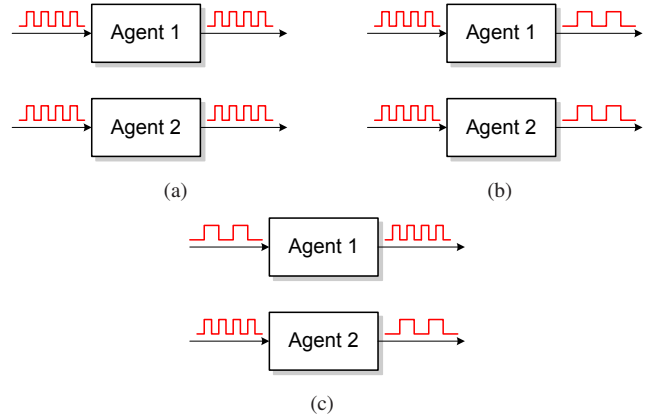


Fig. 1. Schematic of a two-agent (a) single-rate system, (b) synchronous multi-rate system, and (c) asynchronous multi-rate system.

In a multi-rate *output* setting, the output vector $\mathbf{y}_i(t)$ of subsystem i can be measured every T_{y_i} time units, where $T_{y_i} > 0$. At those sampling time instants at which the measurements are not available, the distributed KF proposed in the next section provides the optimal estimation of the missing measurements. Define the switching function γ_{i_j} , for $j = 1, 2, \dots, q_i$ with q_i being the number of outputs of subsystem i , as follows:

$$\gamma_{i_j}(t) = \begin{cases} 1 & \text{if } t = \tau_{y_j}T_{y_j}, \text{ for some integer } \tau_{y_j} \\ 0 & \text{otherwise,} \end{cases} \quad (3)$$

The following measured output vector $\boldsymbol{\varphi}_i(t)$ can now be defined:

$$\boldsymbol{\varphi}_i(t) = \boldsymbol{\Upsilon}_i(t)\mathbf{y}_i(t), \quad (4)$$

where

$$\boldsymbol{\Upsilon}_i(t) = \text{diag}[\gamma_{i_1}(t), \gamma_{i_2}(t), \dots, \gamma_{i_{q_i}}(t)]. \quad (5)$$

In a multi-rate *input* setting, the input vector $\mathbf{u}_i(t)$ of subsystem i is updated every T_{u_i} time units, where $T_{u_i} > 0$. As the input updating happens occasionally, updating the state-space model, which requires the input computation at each sampling time, may lead us to faulty estimation. This problem can be solved by substituting the estimated states obtained by the proposed distributed KF. Introduce a switching function μ_{i_j} for $j = 1, 2, \dots, l_i$ with l_i being the number of inputs of subsystem i . Define the inputs holding mechanism as:

$$\mu_{i_j}(t) = \begin{cases} 1 & \text{if } t = \tau_{u_j} T_{u_j}, \text{ for some integer } \tau_{u_j} \\ 0 & \text{otherwise,} \end{cases} \quad (6)$$

The following input matrix $\Psi_i(t)$ for subsystem i can be defined:

$$\Psi_i(t) = \text{diag}[\mu_{i_1}(t), \mu_{i_2}(t), \dots, \mu_{i_{l_i}}(t)]. \quad (7)$$

Now a new control variable $\boldsymbol{\vartheta}_i(t)$ is introduced to implement the input administering mechanism:

$$\Delta \mathbf{u}_i(t) = \Psi_i(t) \boldsymbol{\vartheta}_i(t). \quad (8)$$

After substituting (8) into (1) and substituting (2) into (4) we obtain:

$$\begin{aligned} \mathbf{x}_i(t+1) &= \mathbf{A}_{ii} \mathbf{x}_i(t) + \mathbf{B}_i \Psi_i(t) \boldsymbol{\vartheta}_i(t) + \mathbf{D}_i \mathbf{v}_i(t) \\ &+ \sum_{\substack{j=1 \\ j \neq i}}^m \mathbf{A}_{ij} \mathbf{x}_j(t), \end{aligned} \quad (9)$$

As in multi-rate systems output measurements are made at specific sampling times, the output sampling mechanism needs to be included in the system's model. To do that both sides of (2) are multiplied by the output sampling parameter $\Upsilon_i(t)$:

$$\Upsilon_i(t) \mathbf{y}_i(t) = \Upsilon_i(t) \mathbf{C}_i \mathbf{x}_i(t) + \Upsilon_i(t) \mathbf{z}_i(t). \quad (10)$$

The left-hand side of (10) can be replaced by (4), therefore:

$$\boldsymbol{\varphi}_i(t) = \Upsilon_i(t) \mathbf{C}_i \mathbf{x}_i(t) + \Upsilon_i(t) \mathbf{z}_i(t). \quad (11)$$

Equations (9) and (11) describe the linear state space model of the distributed multi-rate system for $i = 1, 2, \dots, m$ with m the number of subsystems. In the following section, a distributed MPC problem will be formulated.

B. Control Methodology

In the distributed control structure, state coupling among subsystems is considered as given by (9). Each subsystem is controlled by a so-called agent. The agents communicate with one another to accomplish a global objective. Each agent i shares both its decided input trajectory provided by the local MPC controller $\boldsymbol{\theta}_i(t)$ and also its estimated state trajectory $\hat{\mathbf{x}}_i(t)$ provided by the local Kalman filter, with the neighboring agents (see Fig. 2). One type of distributed MPC is based on Nash optimality [8], [9]. In this approach, the agents communicate with one another, but they do not take a cooperative decision. This means that agents do not have knowledge about other agents' objectives and they use the optimal values provided by the neighboring agents to make their optimal decision. An initial guess for each agent is first

given based on the solution found at the last sampling time. The agents then iterate to resolve their local optimization problem simultaneously and obtain their locally optimal solution [9]. Then each agent checks if its terminal iteration condition satisfies a user-defined threshold. This implies that the agents do not share information about the utility of each decision. Agreement (Nash equilibrium) between the agents has been reached when neither of the agents can improve its solution. In other words, in Nash-based MPC each agent transmits current state and input trajectory information to all interconnected subsystems' MPCs. Competing agents have no knowledge of each others cost functions. From a game theoretic perspective, the equilibrium of such a strategy, if it exists, is called a noncooperative equilibrium or Nash equilibrium [7]. The main advantage of this scheme is that the on-line optimization of a large-scale problem can be converted into several small-scale subproblems, thus reducing the computational complexity significantly while keeping satisfactory performance in the presence of noise and disturbances [31]. Similar strategies have been proposed in [32]. An open-loop Nash equilibrium solution has been studied in [33]. In [34] Nash equilibrium solutions has been proposed for stochastic dynamic games. In this paper we develop a Nash-based MPC for distributed multi-rate systems.

Consider a linear system consisting of m subsystems and m

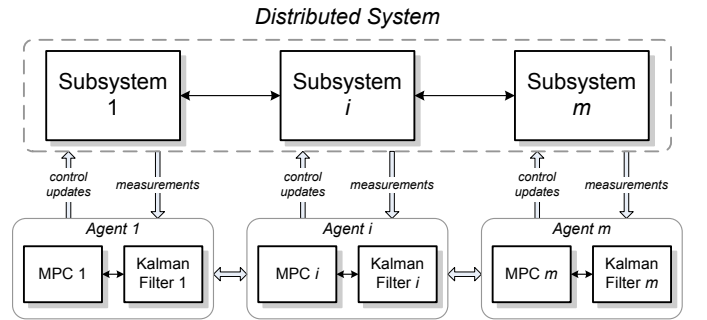


Fig. 2. Distributed MPC control and distributed KF estimation structure.

control agents. In Nash-based distributed MPC each control agent calculates the manipulated variable $\boldsymbol{\vartheta}_i(t)$ by minimizing its local cost function as follows:

$$\begin{aligned} \min_{\boldsymbol{\vartheta}_i(t), \dots, \boldsymbol{\vartheta}_i(t+N_c-1)} J_i(t) &= \sum_{k=1}^{N_p} \|\mathbf{y}_i(t+k) - \mathbf{y}_i^0(t+k)\|_{\mathbf{Q}_i}^2 \\ &+ \sum_{k=0}^{N_c-1} \|\boldsymbol{\vartheta}_i(t+k)\|_{\mathbf{R}_i}^2, \end{aligned} \quad (12)$$

subject to

$$\boldsymbol{\vartheta}_{i,\min} \leq \boldsymbol{\vartheta}_i(t+k) \leq \boldsymbol{\vartheta}_{i,\max}, \quad k = 0, 1, \dots, N_c-1, \quad (13)$$

$$\bar{\mathbf{G}}_i \mathbf{y}_i(t+k) \leq 0 \quad k = 1, 2, \dots, N_p, \quad (14)$$

$$\begin{aligned} \mathbf{x}_i(t+k+1) &= \mathbf{A}_{ii} \mathbf{x}_i(t+k) + \mathbf{B}_i \Psi_i(t+k) \boldsymbol{\vartheta}_i(t+k) \\ &+ \mathbf{D}_i \mathbf{v}_i(t+k) + \sum_{\substack{j=1 \\ j \neq i}}^m \mathbf{A}_{ij} \mathbf{x}_j(t+k), \quad k = 0, 1, \dots, N_p-1, \end{aligned} \quad (15)$$

where $\bar{\mathbf{G}}_i$ is a constant matrix and $\bar{\mathbf{G}}_i \mathbf{y}_i$ represents a set of inequality constraints on the states. Also, $\boldsymbol{\vartheta}_i(t+k) = 0$, for $k = N_c, \dots, N_p - 1$. The variables $\boldsymbol{\vartheta}_{i,\min}$ and $\boldsymbol{\vartheta}_{i,\max}$ are the lower and upper bounds for the inputs, respectively, $\mathbf{Q}_i \geq 0$ and $\mathbf{R}_i > 0$ denote the weighting matrices, and N_p and N_c are the prediction and control horizons, respectively. The set-point is denoted by \mathbf{y}_i^0 and notation $\|\mathbf{y}\|_Q$ defines the weighted Euclidean norm, i.e. $\|\mathbf{y}\|_Q^2 = \mathbf{y}^T \mathbf{Q} \mathbf{y}$. In order to solve the problem in (12)–(15), first we substitute (9) into (2). Based on the obtained state-space model the future state variables are then calculated sequentially using the set of future control variables $\boldsymbol{\theta}_i(t)$. The matrices thus obtained can be written in a compact form given by,

$$\mathbf{Y}_i(t) = \mathbf{F}_i \mathbf{x}_i(t) + \boldsymbol{\phi}_{ii}(t) \boldsymbol{\theta}_i(t) + \boldsymbol{\Gamma}_i \boldsymbol{\zeta}_i(t) + \sum_{\substack{j=1 \\ j \neq i}}^m \mathbf{X}_j(t) \boldsymbol{\phi}_{ij}(t), \quad (16)$$

with

$$\mathbf{Y}_i(t) = [\mathbf{y}_i^T(t+1) \ \mathbf{y}_i^T(t+2) \ \dots \ \mathbf{y}_i^T(t+N_p)]^T, \quad (17)$$

$$\boldsymbol{\theta}_i(t) = [\boldsymbol{\vartheta}_i^T(t) \ \boldsymbol{\vartheta}_i^T(t+1) \ \dots \ \boldsymbol{\vartheta}_i^T(t+N_c-1)]^T, \quad (18)$$

$$\mathbf{X}_j(t) = [\mathbf{x}_j^T(t) \ \mathbf{x}_j^T(t+1) \ \dots \ \mathbf{x}_j^T(t+N_p-1)]^T, \quad (19)$$

$$\boldsymbol{\zeta}_i(t) = [\mathbf{v}_i^T(t) \ \mathbf{v}_i^T(t+1) \ \dots \ \mathbf{v}_i^T(t+N_c-1)]^T, \quad (20)$$

$$\mathbf{F}_i = [(\mathbf{C}_i \mathbf{A}_{ii})^T \ (\mathbf{C}_i \mathbf{A}_{ii}^2)^T \ \dots \ (\mathbf{C}_i \mathbf{A}_{ii}^{N_p})^T]^T, \quad (21)$$

$$\boldsymbol{\phi}_{ii}(t) = \begin{bmatrix} \mathbf{C}_i \mathbf{B}_i \boldsymbol{\Psi}_i(t) & 0 & \dots & 0 \\ \mathbf{C}_i \mathbf{A}_{ii} \mathbf{B}_i \boldsymbol{\Psi}_i(t) & \vdots & \ddots & \vdots \\ \vdots & \vdots & \vdots & 0 \\ \mathbf{C}_i \mathbf{A}_{ii}^{N_p-1} \mathbf{B}_i \boldsymbol{\Psi}_i(t) & \dots & \dots & \mathbf{C}_i \mathbf{A}_{ii}^{N_p-N_c} \mathbf{B}_i \boldsymbol{\Psi}_i(t+N_c-1) \end{bmatrix}, \quad (22)$$

$$\boldsymbol{\Gamma}_i = \begin{bmatrix} \mathbf{C}_i \mathbf{D}_i & 0 & \dots & 0 \\ \mathbf{C}_i \mathbf{A}_{ii} \mathbf{D}_i & \mathbf{C}_i \mathbf{D}_i & \ddots & \vdots \\ \vdots & \vdots & \vdots & 0 \\ \mathbf{C}_i \mathbf{A}_{ii}^{N_p-1} \mathbf{D}_i & \mathbf{C}_i \mathbf{A}_{ii}^{N_p-2} \mathbf{D}_i & \dots & \mathbf{C}_i \mathbf{A}_{ii}^{N_p-N_c} \mathbf{D}_i \end{bmatrix}, \quad (23)$$

$$\boldsymbol{\phi}_{ij}(t) = \begin{bmatrix} \mathbf{C}_i \mathbf{A}_{ij} & 0 & \dots & 0 \\ \mathbf{C}_i \mathbf{A}_{ii} \mathbf{A}_{ij} & \vdots & \ddots & \vdots \\ \vdots & \vdots & \vdots & 0 \\ \mathbf{C}_i \mathbf{A}_{ii}^{N_p-1} \mathbf{A}_{ij} & \dots & \dots & \mathbf{C}_i \mathbf{A}_{ii}^{N_p-N_c} \mathbf{A}_{ij} \end{bmatrix}. \quad (24)$$

In (20), we assumed that the process noise is zero from $t + N_c - 1$ on: $\mathbf{v}_i(t+k) = 0$ for $k = N_c, \dots, N_p - 1$.

In practice, the current state of each subsystem $\mathbf{x}_i(t)$ and also the current state of the neighboring subsystems $\mathbf{x}_j(t)$ are usually not available from measurements in a multi-rate system and a state observer needs to be used to reconstruct the full state vector. In this case, we replace $\mathbf{x}_i(t)$ and $\mathbf{x}_j(t)$

by their estimates $\hat{\mathbf{x}}_i(t)$ and $\hat{\mathbf{x}}_j(t)$, resulting in:

$$\hat{\mathbf{Y}}_i(t) = \mathbf{F}_i \hat{\mathbf{x}}_i(t) + \boldsymbol{\phi}_{ii}(t) \boldsymbol{\theta}_i(t) + \boldsymbol{\Gamma}_i \boldsymbol{\zeta}_i(t) + \sum_{\substack{j=1 \\ j \neq i}}^m \hat{\mathbf{X}}_j(t) \boldsymbol{\phi}_{ij}(t), \quad (25)$$

where $\hat{\mathbf{X}}_j(t) = [\hat{\mathbf{x}}_j^T(t) \ \hat{\mathbf{x}}_j^T(t+1) \ \dots \ \hat{\mathbf{x}}_j^T(t+N_p-1)]^T$ is the vector of estimated states over the prediction horizon of the neighboring subsystems and is provided by the multi-rate estimator that will be introduced in the next section. If $\mathbf{Y}_i^0(t) = [\mathbf{y}_i^{0T}(t+1) \ \mathbf{y}_i^{0T}(t+2) \ \dots \ \mathbf{y}_i^{0T}(t+N_p)]^T$, the local optimization problem (12) for agent i can be reformulated as:

$$\min_{\boldsymbol{\theta}_i(t)} J_i(\hat{\mathbf{x}}_i(t), \hat{\mathbf{X}}_{j \neq i}(t), \boldsymbol{\theta}_i(t)) = \|\hat{\mathbf{Y}}_i(t) - \mathbf{Y}_i^0(t)\|_{\bar{\mathbf{Q}}_i}^2 + \|\boldsymbol{\theta}_i(t)\|_{\bar{\mathbf{R}}_i}^2, \quad (26)$$

$$\text{subject to } \boldsymbol{\theta}_{i,\min} \leq \boldsymbol{\theta}_i(t) \leq \boldsymbol{\theta}_{i,\max}, \quad (27)$$

$$\mathbf{G}_i \hat{\mathbf{Y}}_i(t) \leq 0, \quad (28)$$

$$\begin{aligned} \hat{\mathbf{x}}_i(t+k+1) &= \mathbf{A}_{ii} \hat{\mathbf{x}}_i(t+k) + \mathbf{B}_i \boldsymbol{\Psi}_i(t+k) \boldsymbol{\theta}_i(t+k) \\ &+ \mathbf{D}_i \mathbf{v}_i(t+k) + \sum_{\substack{j=1 \\ j \neq i}}^m \mathbf{A}_{ij} \hat{\mathbf{x}}_j(t+k), \quad k = 0, 1, \dots, N_p-1, \end{aligned} \quad (29)$$

where \mathbf{G}_i is a matrix reflecting the constraints with its number of rows equal to the number of constraints and number of columns equal to the dimension of \mathbf{Y}_i . Also, $\bar{\mathbf{Q}}_i = \text{diag}[\mathbf{Q}_i, \dots, \mathbf{Q}_i]$ and $\bar{\mathbf{R}}_i = \text{diag}[\mathbf{R}_i, \dots, \mathbf{R}_i]$ are the block-diagonal output and input weight matrices, respectively. The lower and upper bounds for the input sequence $\boldsymbol{\theta}_i(t)$ are denoted by $\boldsymbol{\theta}_{i,\min}$ and $\boldsymbol{\theta}_{i,\max}$, respectively. It can be shown [30] that problem (26)–(29) is equivalent to a quadratic programming problem, which can be solved efficiently and reliably using standard off-the-shelf solvers.

The optimization problem (26)–(29) is solved iteratively using Nash-based MPC. The Nash-based MPC algorithm for solving the control problem proceeds by allowing each subsystem to optimize its objective function using its own control decision $\boldsymbol{\vartheta}_i(t)$ assuming that neighboring subsystem solutions $\boldsymbol{\vartheta}_j(t)$ are known. Let $\boldsymbol{\vartheta}_i^n(t)$ define the computed control input for subsystem i at iteration n , ($n \geq 0$). At each sampling time step each agent makes an initial guess of its decision variables over the control horizon and broadcasts that to the neighboring agents:

$$\boldsymbol{\theta}_i^n(t) = [(\boldsymbol{\vartheta}_i^n(t))^T \ (\boldsymbol{\vartheta}_i^n(t+1))^T \ \dots \ (\boldsymbol{\vartheta}_i^n(t+N_c-1))^T]^T, \quad (30)$$

Then, each agent solves its optimization problem (26)–(29) and gets its optimal solution $\boldsymbol{\theta}_i^{n+1}(t)$. Next, all the agents compare the new solution $\boldsymbol{\theta}_i^{n+1}(t)$ with the solution obtained at the previous iteration $\boldsymbol{\theta}_i^n(t)$ and check the convergence condition:

$$\|\boldsymbol{\theta}_i^{n+1}(t) - \boldsymbol{\theta}_i^n(t)\| \leq \epsilon, \quad (31)$$

in which ϵ is the error accuracy. When (31) is satisfied, the Nash optimal solution has been achieved. Then each agent

does not change its decision $\boldsymbol{\theta}_i^n(t)$ anymore because it has achieved an equilibrium point of the coupling decision process [31]. The iterations then stop, as otherwise the local cost function $J_i(t)$ will degrade.

Reformulating the objective function in (26) in terms of $\boldsymbol{\theta}_i(t)$ to make the problem applicable for quadratic programming (QP) [30] leads us to:

$$J_i(t) = \frac{1}{2} \boldsymbol{\theta}_i^T(t) [2\boldsymbol{\Phi}_{ii}^T(t)\bar{\mathbf{Q}}_i\boldsymbol{\Phi}_{ii}(t) + 2\bar{\mathbf{R}}_i] \boldsymbol{\theta}_i(t) + 2\hat{\boldsymbol{\Pi}}_i^T \bar{\mathbf{Q}}_i \boldsymbol{\Phi}_{ii}(t) \boldsymbol{\theta}_i(t), \quad (32)$$

where $\hat{\boldsymbol{\Pi}}_i = \left[\mathbf{F}_i \hat{\mathbf{x}}_i(t) + \Gamma_i \boldsymbol{\zeta}_i(t) + \sum_{\substack{j=1 \\ j \neq i}}^m \hat{\mathbf{X}}_j(t) \boldsymbol{\Phi}_{ij}(t) - \mathbf{Y}_i^0(t) \right]$, is a constant for the optimization problem based on the Nash iterative setting. To solve the optimization problem of minimizing (32) subject to the constraints defined in (27)–(29), the following change needs to be applied. Since in the presented cost function in (32), the variable $\hat{\mathbf{Y}}_i(t)$ has been eliminated, the constraint in (28) should be replaced in terms of $\boldsymbol{\theta}_i(t)$,

$$\mathbf{G}_i \left[\mathbf{F}_i \hat{\mathbf{x}}_i(t) + \boldsymbol{\Phi}_{ii}(t) \boldsymbol{\theta}_i(t) + \Gamma_i \boldsymbol{\zeta}_i(t) + \sum_{\substack{j=1 \\ j \neq i}}^m \hat{\mathbf{X}}_j(t) \boldsymbol{\Phi}_{ij}(t) \right] \leq 0. \quad (33)$$

Considering the definition of $\hat{\boldsymbol{\Pi}}_i$, (33) can be written as:

$$\mathbf{G}_i \left[\boldsymbol{\Phi}_{ii}(t) \boldsymbol{\theta}_i(t) + \hat{\boldsymbol{\Pi}}_i + \mathbf{Y}_i^0(t) \right] \leq 0. \quad (34)$$

Now, (27) and (34) can be combined as:

$$\begin{bmatrix} \boldsymbol{\Phi}_{ii}(t) \\ \mathbf{I} \\ -\mathbf{I} \end{bmatrix} \boldsymbol{\theta}_i(t) \leq \begin{bmatrix} -\hat{\boldsymbol{\Pi}}_i - \mathbf{Y}_i^0(t) \\ \boldsymbol{\theta}_{i,\max} \\ -\boldsymbol{\theta}_{i,\min} \end{bmatrix}. \quad (35)$$

Hence, in general the optimization problem in (32) can be solved subject to the overall constraints defined by (35).

On the other hand from the augmented model in (9), the variable $\boldsymbol{\theta}_i$ is the increment of the real input, therefore we need to transform the constraints on the rate of the inputs to the constraints on the inputs themselves. To do so, consider (8), in which we have:

$$\boldsymbol{\Psi}_i(t) = 0 \rightarrow \Delta \mathbf{u}_i(t) = 0, \quad (36)$$

$$\boldsymbol{\Psi}_i(t) = 1 \rightarrow \Delta \mathbf{u}_i(t) = \boldsymbol{\theta}_i(t). \quad (37)$$

Considering (37), the constraints in (27) can be written as:

$$\Delta \mathbf{u}_{i,\min} \leq \Delta \mathbf{u}_i(t) \leq \Delta \mathbf{u}_{i,\max}. \quad (38)$$

Now, consider (38) over the control horizon,:

$$-\Delta \mathbf{U}_i(t) \leq -\Delta \mathbf{U}_{i,\min}, \quad (39)$$

$$\Delta \mathbf{U}_i(t) \leq \Delta \mathbf{U}_{i,\max}, \quad (40)$$

where $\Delta \mathbf{U}_i(t) = [\Delta \mathbf{u}_i^T(t), \Delta \mathbf{u}_i^T(t+1), \dots, \Delta \mathbf{u}_i^T(t+N_c-1)]^T$, and $\Delta \mathbf{U}_{i,\min}$ and $\Delta \mathbf{U}_{i,\max}$ are column vectors with N_c elements of $\Delta \mathbf{u}_{i,\min}$ and $\Delta \mathbf{u}_{i,\max}$, respectively.

Equations (39) and (40) in a compact form can be expressed as:

$$\begin{bmatrix} -\mathbf{I} \\ \mathbf{I} \end{bmatrix} \Delta \mathbf{U}_i(t) \leq \begin{bmatrix} -\Delta \mathbf{U}_{i,\min} \\ \Delta \mathbf{U}_{i,\max} \end{bmatrix}. \quad (41)$$

Considering the notation $\mathbf{u}_i(t) = \mathbf{u}_i(t-1) + \Delta \mathbf{u}_i(t)$, we can write:

$$\begin{bmatrix} \mathbf{u}_i(t) \\ \mathbf{u}_i(t+1) \\ \vdots \\ \mathbf{u}_i(t+N_c-1) \end{bmatrix} = \begin{bmatrix} \mathbf{I} \\ \mathbf{I} \\ \vdots \\ \mathbf{I} \end{bmatrix} \mathbf{u}_i(t-1) + \begin{bmatrix} \mathbf{I} & 0 & 0 & \cdots & 0 \\ \mathbf{I} & \mathbf{I} & 0 & \cdots & 0 \\ \vdots & \vdots & \vdots & \ddots & \vdots \\ \mathbf{I} & \mathbf{I} & \mathbf{I} & \cdots & \mathbf{I} \end{bmatrix} \begin{bmatrix} \Delta \mathbf{u}_i(t) \\ \Delta \mathbf{u}_i(t+1) \\ \vdots \\ \Delta \mathbf{u}_i(t+N_c-1) \end{bmatrix}. \quad (42)$$

Rewriting (41) and (42) in a compact matrix form, with \mathbf{C}_1 and \mathbf{C}_2 corresponding to the appropriate matrices, then the constraints for the control inputs are imposed as:

$$-(\mathbf{C}_1 \mathbf{u}_i(t-1) + \mathbf{C}_2 \Delta \mathbf{U}_i(t)) \leq -\mathbf{U}_{i,\min}, \quad (43)$$

$$(\mathbf{C}_1 \mathbf{u}_i(t-1) + \mathbf{C}_2 \Delta \mathbf{U}_i(t)) \leq \mathbf{U}_{i,\max}. \quad (44)$$

Using (43) and (44) the constraints on the input increment can be transformed to the constraints on the input itself and vice versa [35].

III. DISTRIBUTED MULTI-RATE KALMAN FILTER

A. Problem Statement

Distributed Kalman filtering [3], [17]–[19] involves state estimation using a set of local Kalman filters that communicate with all other agents. However, in multi-rate state estimation an additional issue needs to be considered which is the multi-rateness of the system. The main issue that is addressed by our proposed method is to introduce a novel state estimation approach for multi-rate linear discrete-time systems in which measurements are only available at certain sampling times.

B. Distributed Multi-Rate Estimation

Consider the linear multi-rate model in (1)–(2). The goal here is to use the available measurements $\boldsymbol{\varphi}_i$ to estimate the state of the system \mathbf{x}_i . Consider the process noise $\mathbf{v}_i(t)$ for subsystem i to be discrete-time white noise signal. The following covariance matrix can hence be defined:

$$\mathbb{E} [\mathbf{v}_i(t) \mathbf{v}_i^T(t)] = \mathbf{S}_{p_i}(t), \quad (45)$$

where $\mathbb{E}[\cdot]$ denotes the expectation of the argument, and $\mathbf{S}_{p_i}(t)$ represents the covariance matrix of the process noise. Consider the measurement noise $\mathbf{z}_i(t)$ in (11) to be discrete-time zero mean white noise. The following covariance matrix for the measurement noise $\mathbf{S}_{m_i}(t)$ can be defined similarly:

$$\mathbb{E} [\mathbf{z}_i(t) \mathbf{z}_i^T(t)] = \mathbf{S}_{m_i}(t). \quad (46)$$

The equations for the proposed KF are divided into two parts: estimation (prediction) equations and measurement update equations.

1) *Prediction*: In the proposed distributed Kalman Filter for the multi-rate system, each local Kalman Filter should estimate $\mathbf{x}_i(t)$ such that the covariance of $\mathbf{x}_i(t) - \widehat{\mathbf{x}}_i(t)$ is minimized, when $\widehat{\mathbf{x}}_i(t)$ is the estimate of $\mathbf{x}_i(t)$. Let the one step-ahead prediction be expressed as follows:

$$\widehat{\mathbf{x}}_i(t+1|t) = \mathbf{A}_{ii}\widehat{\mathbf{x}}_i(t|t-1) + \mathbf{B}_{ii}\Delta\mathbf{u}_i(t) + \sum_{\substack{j=1 \\ j \neq i}}^m \mathbf{A}_{ij}\widehat{\mathbf{x}}_j(t|t-1), \quad (47)$$

where the index $(t|t-1)$ refers to the information at sampling time t given knowledge of the process prior to sampling time t . The variable $\widehat{\mathbf{x}}_j$ indicates the estimated states of agent j . In this way, exchanging information among agents are done through provided neighboring agents estimation $\widehat{\mathbf{x}}_j$.

The distributed multi-rate Kalman filter equation with \mathbf{L}_i and \mathbf{L}_j as *Kalman Gains* for subsystem i and subsystems $j(j \neq i)$, can be expressed as:

$$\begin{aligned} \widehat{\mathbf{x}}_i(t+1|t) &= \mathbf{A}_{ii}\widehat{\mathbf{x}}_i(t|t-1) + \mathbf{B}_{ii}\Delta\mathbf{u}_i(t) \\ &+ \mathbf{L}_i(t) [\boldsymbol{\varphi}_i(t) - \boldsymbol{\Upsilon}_i(t)\mathbf{C}_i(t)\widehat{\mathbf{x}}_i(t|t-1)] \\ &+ \sum_{\substack{j=1 \\ j \neq i}}^m \mathbf{A}_{ij}\widehat{\mathbf{x}}_j(t|t-1) \\ &+ \mathbf{L}_j(t) [\boldsymbol{\varphi}_j(t) - \boldsymbol{\Upsilon}_j(t)\mathbf{C}_j(t)\widehat{\mathbf{x}}_j(t|t-1)], \quad (48) \end{aligned}$$

Equation (48) is used to compute the vector of estimated states over the prediction horizon for each agent $\widehat{\mathbf{x}}_j(t)$. As it can be seen from (48), each agent computes its estimated states by using its neighboring agents' estimated states $\widehat{\mathbf{x}}_j(t|t-1)$, which have been provided at the prior time step. In other words, local Kalman filters share their estimated states and also their Kalman gain with their neighboring agents. Let the $\mathbf{S}_i(t|t-1)$ be the predicted estimate covariance at sampling time t given observations up to, and including at time $t-1$ then we have:

$$\begin{aligned} \mathbf{S}_i(t|t-1) &= \mathbf{A}_{ii}\widehat{\mathbf{x}}_i(t-1|t-1)\mathbf{A}_{ii}^T + \mathbf{D}_i\mathbf{S}_{p_i}(t)\mathbf{D}_i^T \\ &+ \sum_{\substack{j=1 \\ j \neq i}}^m \mathbf{A}_{ij}\widehat{\mathbf{x}}_j(t-1|t-1)\mathbf{A}_{ij}^T. \quad (49) \end{aligned}$$

These predicted state estimates $\widehat{\mathbf{x}}_i(t|t-1)$ and covariance estimates $\mathbf{S}_i(t|t-1)$ are in fact an estimation at the current sampling time and they do not include observation information from the current sampling time. In the update phase, the current prediction is combined with current observation information to refine the state estimation.

2) *Measurement Update*: Define the innovation or measurement residual for each subsystem i as,

$$\boldsymbol{\Lambda}_i(t) = \mathbf{y}_i(t) - \mathbf{C}_i(t)\widehat{\mathbf{x}}_i(t|t-1). \quad (50)$$

For a multi-rate system the estimated state is introduced by replacing $\mathbf{y}_i(t)$ with $\boldsymbol{\varphi}_i(t)$ in (11). Note that all \mathbf{C}_i matrices are replaced by $\boldsymbol{\Upsilon}_i(t)\mathbf{C}_i$. Applying this, (50) can be represented as,

$$\boldsymbol{\Upsilon}_i(t)\boldsymbol{\Lambda}_i(t) = \boldsymbol{\varphi}_i(t) - \boldsymbol{\Upsilon}_i(t)\mathbf{C}_i(t)\widehat{\mathbf{x}}_i(t|t-1). \quad (51)$$

The modified innovation covariance is then defined as follows:

$$\begin{aligned} \boldsymbol{\Omega}_i(t) &= \boldsymbol{\Upsilon}_i(t)\mathbf{C}_i\mathbf{S}_i(t|t-1)\mathbf{C}_i^T\boldsymbol{\Upsilon}_i(t) + \boldsymbol{\Upsilon}_i(t)\mathbf{S}_{m_i}(t)\boldsymbol{\Upsilon}_i(t) \\ &+ [\mathbf{I}_{q \times q} - \boldsymbol{\Upsilon}_i(t)]. \quad (52) \end{aligned}$$

In order to guarantee that $\boldsymbol{\Omega}_i(t)$ is non-singular at any time instant, the extra term $[\mathbf{I}_{q \times q} - \boldsymbol{\Upsilon}_i(t)]$ has been added to (52), in which $\mathbf{I}_{q \times q}$ is the identity matrix of size q by q [20]. The matrix $\boldsymbol{\Omega}_i(t)$ is block diagonal and the matrix $[\mathbf{I}_{q \times q} - \boldsymbol{\Upsilon}_i(t)]$ only adds non-zero terms to the scalar diagonal elements of $\boldsymbol{\Omega}_i(t)$ during the output sampling mechanism when there are no measurements available (the output sampling mechanism described by $\boldsymbol{\Upsilon}_i(t)$ is zero). Therefore, adding $[\mathbf{I}_{q \times q} - \boldsymbol{\Upsilon}_i(t)]$ to (52) in no way affects the estimator.

Introducing the *Kalman Gain* for the multi-rate system as:

$$\mathbf{L}_i(t) = \mathbf{A}_{ii}\mathbf{S}_i(t|t-1)\mathbf{C}_i^T\boldsymbol{\Upsilon}_i(t)\boldsymbol{\Omega}_i^{-1}(t), \quad (53)$$

we proceed to update the estimation error covariance considering (9) and (47) as:

$$\mathbf{e}_i(t+1|t) = \mathbf{x}_i(t+1|t) - \widehat{\mathbf{x}}_i(t+1|t). \quad (54)$$

By substituting (11) into (51) and then proceeding by substituting it along with (9) and (47) into (54) we obtain:

$$\begin{aligned} \mathbf{S}_i(t+1|t) &= \text{cov}[\mathbf{e}_i(t+1|t)] \\ &= \text{cov}[(\mathbf{A}_{ii} - \mathbf{L}_i(t)\boldsymbol{\Upsilon}_i(t)\mathbf{C}_i)\mathbf{e}_i(t|t-1) \\ &+ \mathbf{D}_i\mathbf{v}_i(t) - \mathbf{L}_i(t)\boldsymbol{\Upsilon}_i(t)\mathbf{z}_i(t) + \sum_{\substack{j=1 \\ j \neq i}}^m \mathbf{A}_{ij}\widehat{\mathbf{x}}_j(t|t-1)]. \quad (55) \end{aligned}$$

Expanding the terms and also considering the properties of the vector covariance [29] we get:

$$\begin{aligned} \mathbf{S}_i(t+1|t) &= \mathbf{A}_{ii}\mathbf{S}_i(t|t-1)\mathbf{A}_{ii}^T - 2\mathbf{L}_i(t)\boldsymbol{\Upsilon}_i(t)\mathbf{C}_i\mathbf{S}_i(t|t-1)\mathbf{A}_{ii}^T \\ &+ \mathbf{L}_i(t)\boldsymbol{\Omega}_i(t)\mathbf{L}_i^T(t) + \mathbf{D}_i\mathbf{S}_{p_i}(t)\mathbf{D}_i^T \\ &+ \sum_{\substack{j=1 \\ j \neq i}}^m \mathbf{A}_{ij}\mathbf{S}_j(t|t-1)\mathbf{A}_{ij}^T. \quad (56) \end{aligned}$$

Minimizing the error covariance with respect to Kalman gain $\mathbf{L}_i(t)$ yields:

$$\begin{aligned} \frac{\partial \mathbf{S}_i(t+1|t)}{\partial \mathbf{L}_i(t)} &= \frac{\partial}{\partial \mathbf{L}_i(t)} [\mathbf{A}_{ii}\mathbf{S}_i(t|t-1)\mathbf{A}_{ii}^T \\ &- 2\mathbf{L}_i(t)\boldsymbol{\Upsilon}_i(t)\mathbf{C}_i\mathbf{S}_i(t|t-1)\mathbf{A}_{ii}^T \\ &+ \mathbf{L}_i(t)\boldsymbol{\Omega}_i(t)\mathbf{L}_i^T(t) + \mathbf{D}_i\mathbf{S}_{p_i}(t)\mathbf{D}_i^T \\ &+ \sum_{\substack{j=1 \\ j \neq i}}^m \mathbf{A}_{ij}\mathbf{S}_j(t|t-1)\mathbf{A}_{ij}^T] = 0. \quad (57) \end{aligned}$$

It should be noted that (56) is the algebraic Riccati equation and from (57) the minimum is attained if and only if [16]:

$$-2\mathbf{A}_{ii}\mathbf{S}_i(t|t-1)\mathbf{C}_i^T\boldsymbol{\Upsilon}_i(t) + 2\mathbf{L}_i(t)\boldsymbol{\Omega}_i(t) = 0. \quad (58)$$

The Kalman filter gain for each subsystem i can be found by solving (52), (53), (56) and (58) iteratively backwards in time.

IV. CASE STUDY

A power system example with two control areas interconnected through a tie line [7] is considered to illustrate the performance of the proposed method. We have selected this example because it is a well-known benchmark that has already been used to study distributed MPC algorithms [36], [7], so it is familiar to the readers. On the one hand the presented example is simple enough to demonstrate our proposed method while on the other hand, it is nontrivial. Most interconnected power systems rely on automatic generation control (AGC) for controlling system frequency and tie-line interchange [7]. These objectives are achieved by regulating the real power output of generators throughout the system. To cope with the expansive nature of power systems, various limits must be taken into account, including restrictions on the amount and rate of generator power deviation. AGC therefore provides a very relevant example for illustrating the performance of distributed multi-rate predictive control and estimation in a power network setting. For the purpose of AGC, power systems are decomposed into control areas, with tie lines providing interconnections between the areas [7]. Each area typically consists of numerous generators and loads. It is common, though, for all generators in an area to be lumped as a single equivalent generator, and likewise for loads. This approach is adopted in the considered case study [7].

A. Two-Area Power System Model and Control Structure

The following nominal normalized state-space continuous-time model for each area i is considered [7]:

$$\frac{d\Delta w_i}{dt} = -\frac{1}{M_i^a}(D_i\Delta w_i + \Delta P_{\text{tie}}^{ij} - \Delta P_{\text{mech}_i} + \Delta P_{L_i}), \quad (59)$$

$$\frac{d\Delta P_{\text{mech}_i}}{dt} = -\frac{1}{T_{\text{CH}_i}}(\Delta P_{\text{mech}_i} - \Delta P_{V_i}), \quad (60)$$

$$\frac{d\Delta P_{V_i}}{dt} = -\frac{1}{T_{G_i}}(\Delta P_{V_i} - \Delta P_{\text{ref}_i} + \frac{1}{R_i^f}\Delta w_i), \quad (61)$$

where the definitions of the power system variables and parameters are provided in Table I. The notation Δ is used to indicate the deviation from steady state. For example, Δw represents the deviation in the angular frequency from its nominal operating value (50 Hz).

The tie-line power flow between areas i and j is expressed as:

$$\frac{d\Delta P_{\text{tie}}^{ij}}{dt} = T_{ij}(\Delta w_i - \Delta w_j), \quad (62)$$

$$\Delta P_{\text{tie}}^{ji} = -\Delta P_{\text{tie}}^{ij}. \quad (63)$$

Since the model is used in the predictive controller synthesis, the load variable ΔP_{L_i} for each area i , as a disturbance input, is assumed constant during predictions, i.e.

$$\frac{d\Delta P_{L_i}}{dt} = 0, \quad i = 1, 2. \quad (64)$$

Each subsystem is connected via state coupling $\Delta P_{\text{tie}}^{12}$. The output (controlled variable) for area 1 is the frequency deviation Δw_1 and the output for area 2 is the deviation in the

TABLE I
BASIC POWER SYSTEM DEFINITION

Parameter	Description
w	Angular frequency
M^a	Angular momentum
D	Ratio of change in load to change in frequency
T_{CH}	Charging time constant
T_{G}	Governor time constant
R^f	Ratio of change in frequency to change in unit output
T_{ij}	Tie-line stiffness coefficient between areas i and j
P_{mech}	Mechanical power
P_L	Non-frequency sensitive load
P_V	Steam valve position
P_{ref}	Load reference set-point
P_{tie}^{ij}	Tie-line power flow between areas i and j

TABLE II
PARAMETERS OF THE TWO-AREA POWER SYSTEM MODEL

Parameter	Area 1	Area 2
D_i	2	2.75
R_i^f	0.03	0.07
M_i^a	3.5	4.0
T_{CH_i}	50	10
T_{G_i}	40	25

tie-line power flow between the two control areas ($\Delta P_{\text{tie}}^{12}$). By examining the power system model (60), it is clear that, if $\Delta\omega_1 \rightarrow 0$ and $\Delta P_{\text{tie}}^{12} \rightarrow 0$ then $\Delta\omega_2 \rightarrow 0$.

Discretizing the process (59)-(64) with a sampling interval of $T_s = 1$ s leads to the discrete-time state-space model (1)-(2) with

$$\mathbf{x}_i = [\Delta\omega_i \quad \Delta P_{\text{mech}_i} \quad \Delta P_{V_i} \quad \Delta P_{L_i} \quad \Delta P_{\text{tie}}^{ij}]^T, \quad (65)$$

$$\mathbf{u}_i = \Delta P_{\text{ref}_i}, \quad (66)$$

$$\mathbf{y}_1 = \Delta\omega_1, \quad \mathbf{y}_2 = \Delta P_{\text{tie}}^{12}. \quad (67)$$

and where matrices \mathbf{A}_{ii} , \mathbf{A}_{ij} , \mathbf{B}_i , \mathbf{C}_i can be easily constructed from (59)-(64). The model parameters are given in Table II. The tie-line stiffness coefficient between area, 1 and 2 is given by $T_{12} = 7.54$.

In Fig. 3, the block diagram of the distributed MPC control structure for the considered power system example is shown. Each control area i consists of a MPC controller that is used to generate optimal load reference set-point ΔP_{ref_i} based on optimal estimated system states computed by the KF.

B. Design of Distributed KF and MPC

The design process for the distributed KF consists of the selection of noise covariance matrices \mathbf{S}_{p_i} and \mathbf{S}_{m_i} for each subsystem i . Needless to say, the estimation quality depends on how accurately these matrices reflect the actual noise conditions in a real system. In this paper, it is assumed that the process and measurement noise signals for both control areas are white noise sequences with covariances $\mathbf{S}_{p_1} = \mathbf{S}_{p_2} = \mathbf{S}_{m_1} = \mathbf{S}_{m_2} = 10^{-5}$. Since the only measurements available in the system are frequency deviations $\Delta\omega_1$ and $\Delta\omega_2$ as well as load reference set-points ΔP_{ref_1} and ΔP_{ref_2} (see Fig. 3), the remaining system states in (65) will be reconstructed by the proposed distributed KF as described in Section III.

The design process for the distributed MPC controller in (12)-(15) consists of the selection of the prediction horizon and

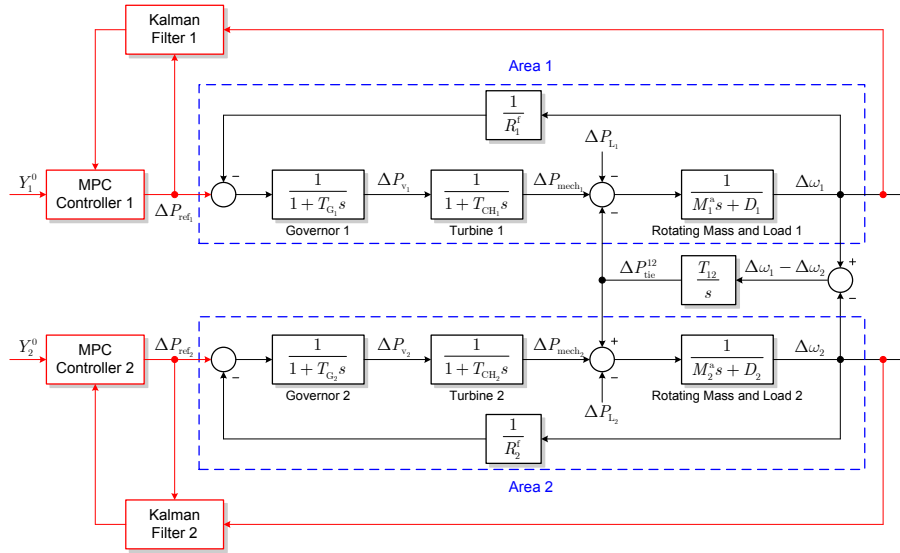


Fig. 3. Block diagram of the two-area interconnected power system control structure.

control horizons N_p and N_c , respectively as well as the output and input weighting matrices \mathbf{Q}_i and \mathbf{R}_i for each control area i such that the desired level of closed-loop performance is achieved. To aid the comparison with other distributed MPC control strategies [7], the prediction and control horizons are chosen as $N_p = 20$ and $N_c = 15$, as suggested in [7].

The input and output weighting matrices for the distributed MPC control problem for both subsystems are chosen as $R_i = \mathbf{I}$ and $Q_i = 5\mathbf{I}$, respectively. A larger output weight relative to the input weight means that it is more important to penalize the frequency and tie-line power imbalance than the load reference deviation from the steady-state value.

While the primary goal of the distributed MPC controller is to provide good frequency and power regulation, the control system must respect the physical and safety limitations of the power system variables during operation. In this paper, the load reference set-point variables in each area are constrained as follows:

$$-0.3 \leq \Delta P_{\text{ref}_i} \leq 0.3, \quad i = 1, 2, \quad (68)$$

where the input as defined in (66) is the deviation of the absolute value of P_{ref_i} with respect to the steady-state value ΔP_{ref_i} . Note that the presented constraints in (68) are constraints on the input itself which is ΔP_{ref_i} , and not on the rate of ΔP_{ref_i} . Therefore in order to apply the proposed algorithm on this example we need to transform the presented constraints in (68) for the rate of ΔP_{ref_i} using (43)–(44).

In the following section, the performance of the proposed distributed multi-rate KF-based MPC control system will be evaluated and compared with the distributed MPC with centralized and decentralized multi-rate Kalman filters.

V. SIMULATION RESULTS

A. Operation Scenarios

Four scenarios are studied to demonstrate the performance of the proposed method. In the two first scenarios, the output

and input for the *synchronous* agents are studied. Then two scenarios consider the *asynchronous* agents (see Fig. 1 for the definition of *asynchronous* and *asynchronous* agents). In the synchronous scenarios each agent is a multi-rate agent which has different input and output sampling rate, however all agents have the same sampling rate in their inputs and outputs as the other agents. In the first considered synchronous scenario, the inputs have a faster sampling rate than the outputs ($T_{u_1} = 1, T_{u_2} = 1, T_{y_1} = 6, T_{y_2} = 6$) and in the second synchronous scenario, a slower input sampling rate has been assumed ($T_{u_1} = 3, T_{u_2} = 3, T_{y_1} = 1, T_{y_2} = 1$).

In the asynchronous scenarios, in addition to agents having different internal sampling rates for their inputs and outputs, these sampling rates will be different for each agent in the system. In the first considered asynchronous case, the inputs have a faster sampling rate than the outputs ($T_{u_1} = 2, T_{u_2} = 3, T_{y_1} = 4, T_{y_2} = 9$) and in the second asynchronous scenario, a slower input sampling rate ($T_{u_1} = 4, T_{u_2} = 3, T_{y_1} = 1, T_{y_2} = 2$) will be considered.

The following performance measure is used to compute the cost of each method as a mean over the complete simulation period T_f :

$$PM = \frac{1}{T_f} \sum_{t=1}^{T_f} \sum_{\substack{i,j=1 \\ j \neq i}}^m J_i^*(\hat{\mathbf{x}}_i(t), \hat{\mathbf{x}}_j(t), \boldsymbol{\theta}_i(t)), \quad (69)$$

The discrepancy of different methods (distributed MPC with distributed multi-rate KF and decentralized multi-rate KF) with respect to centralized MPC with centralized KF is computed as:

$$\Delta PM = \frac{PM_{(\text{method})} - PM_{(\text{centralized})}}{PM_{(\text{centralized})}} 100\%. \quad (70)$$

In all simulation cases, a 15% load disturbance in Area 2 is applied at $t = 5\text{s}$. In order to evaluate the noise filtering properties of the proposed KF algorithm, all measurements

TABLE III
PERFORMANCE COMPARISON AND ANALYSIS FOR *synchronous* AGENTS.

Method	Sampling [s]				PM	ΔPM
	T_{u_1}	T_{u_2}	T_{y_1}	T_{y_2}		
Centralized KF	1	1	6	6	0.1129	0
Proposed DKF	1	1	6	6	0.1174	3.98
Decentralized KF	1	1	6	6	0.2014	78.39
Centralized KF	3	3	1	1	0.4935	0
Proposed DKF	3	3	1	1	0.5092	3.18
Decentralized KF	3	3	1	1	0.8385	69.90

TABLE IV
PERFORMANCE COMPARISON AND ANALYSIS FOR *asynchronous* AGENTS.

Method	Sampling [s]				PM	ΔPM
	T_{u_1}	T_{u_2}	T_{y_1}	T_{y_2}		
Centralized KF	2	3	4	9	0.2810	0
Proposed DKF	2	3	4	9	0.3059	8.86
Decentralized KF	2	3	4	9	0.6245	122.24
Centralized KF	4	3	1	2	0.7521	0
Proposed DKF	4	3	1	2	0.7935	5.50
Decentralized DKF	4	3	1	2	0.8901	18.34

and state variables are perturbed with uniformly distributed random signals of magnitude 10^{-7} .

B. Synchronous Agent Case

In Fig. 4, the simulation results corresponding to the case where the input sampling rate for both agents (power areas) is 6 times faster than the output sampling rate, are presented. It can be observed that the performance of the proposed multi-rate KF method is close to that of the single-rate (perfect) case; the total simulated performance loss ΔPM is 3.98% in comparison to 78.39% in the fully decentralized KF case (see Table III). This means that the multi-rate KF algorithm is more effective in compensating for the information loss due to the infrequent output measurements. Notice that the constraints on the load reference set-point variables imposed in (68) are respected at all times during operation of the controller.

In the second scenario, the input sampling rate is considered to be 3 times slower than the output measurement rate. In Fig. 5, the transient responses of the proposed KF-based MPC control system are depicted. Comparing the results to those in Fig. 4 it is clear that the infrequent input sampling has a greater influence on the closed-loop performance. While the transient behavior in frequency deviation in Area 1 is similar in both cases, the tie-line power flow between the two areas is significantly affected when a slower update rate for inputs ΔP_{ref_1} and ΔP_{ref_2} is considered. This effect is also evident from the transient response of the load reference set-point (input) for Area 1 (Fig. 5(c)); the response is more oscillatory and takes significantly more time to settle. Table III reports that the proposed multi-rate KF method yields smaller deviation from the centralized KF ($\Delta PM = 3.18\%$) in comparison with the decentralized KF ($\Delta PM = 69.90\%$).

C. Asynchronous Agent Scenario

In this section, the two control areas have been considered to be asynchronous in the sense that the input sampling rates

are (i) different for both areas and (ii) faster than the output sampling rates. From the results shown in Fig. 6, it can be seen that the frequency deviation $\Delta\omega_1$ in Area 1 and the tie-line power flow ΔP_{tie}^{12} show smaller deviation from the steady-state for the proposed multi-rate KF compared to the decentralized case. This can be confirmed from the performance metrics reported in Table IV demonstrating that the proposed method results in a lower discrepancy with respect to the centralized KF ($\Delta PM = 8.86\%$) in comparison with the decentralized KF ($\Delta PM = 122.24\%$).

In Fig. 7, the asynchronous control areas having a slower input update rate with respect to the output sampling rate have been studied. Similarly as in the synchronous agent case (Fig. 5), a considerable loss in the closed-loop performance can be noticed. Nevertheless, the system output responses corresponding to the proposed KF method converge slightly faster than for the decentralized KF. Evaluating the performance measure in (69)-(70) for each method, one can find (see Table IV) that the proposed method yields a lower discrepancy with respect to the centralized KF ($\Delta PM = 5.50\%$) in comparison with the decentralized KF ($\Delta PM = 18.34\%$).

VI. CONCLUSIONS AND FUTURE WORK

In this paper, a new Kalman filter-based distributed model predictive control algorithm has been proposed for multi-rate large-scale systems. The proposed framework consists of two main parts, control and estimation. In the control part, a distributed MPC via a Nash game has been studied for multi-rate sampled-data systems and in the estimation part a distributed Kalman Filter (KF) has been proposed to provide the state values for inter-sampling times. The algorithm provides a reliable control and estimation and compensation mechanism for the information loss due to the multi-rate nature of the systems using the proposed distributed KF. In a simulation study involving a two-area power system the proposed method has been compared with a single-rate KF (in plots), centralized KF (in tables) scheme and also with a decentralized multi-rate KF demonstrating significant levels of performance improvement. Several simulation scenarios including slow and fast input sampling as well as slow and fast output sampling in both synchronous and asynchronous arrangements have been considered showing feasibility and high effectiveness.

In the presented method, each agent has knowledge of its own dynamics and also is aware of the neighboring agents' computed inputs. The presented method uses a communication-based optimization based on a Nash Equilibrium, which is non-cooperative and could be unstable [36]. The best achievable performance is characterized by a Pareto set, which represents the set of optimal trade-offs among the competing controller objectives. To cover this drawback more research needs to be done on cooperative MPC algorithms for multi-rate systems. Further research is also needed to prove convergence and stability issues of the proposed method. Another open problem is the development of efficient distributed multi-rate control and estimation approaches that are robust to system parameter variation and model uncertainty.

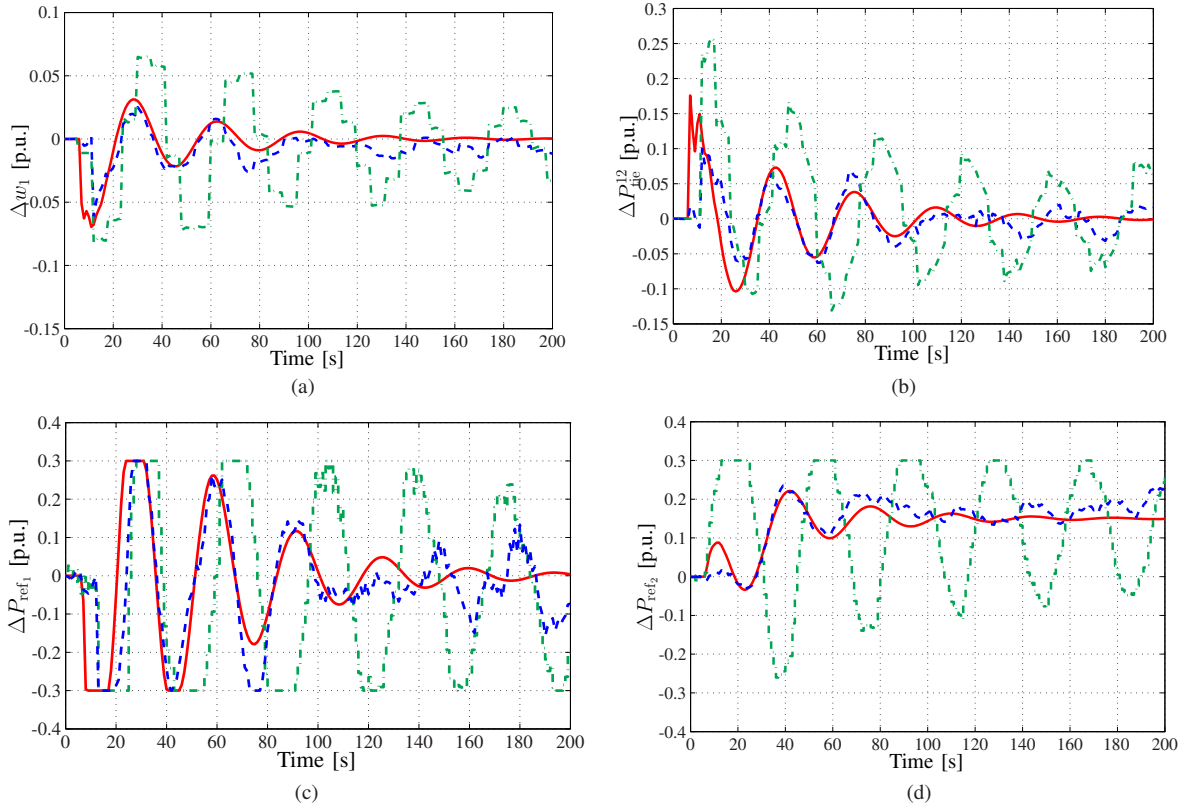


Fig. 4. Closed-loop responses of *synchronous* agents with *faster input / slower output* sampling rates using single-rate KF in red (solid); proposed distributed MPC with multi-rate KF in blue (dashed); distributed MPC with multi-rate decentralized KF in green (dash-dotted).

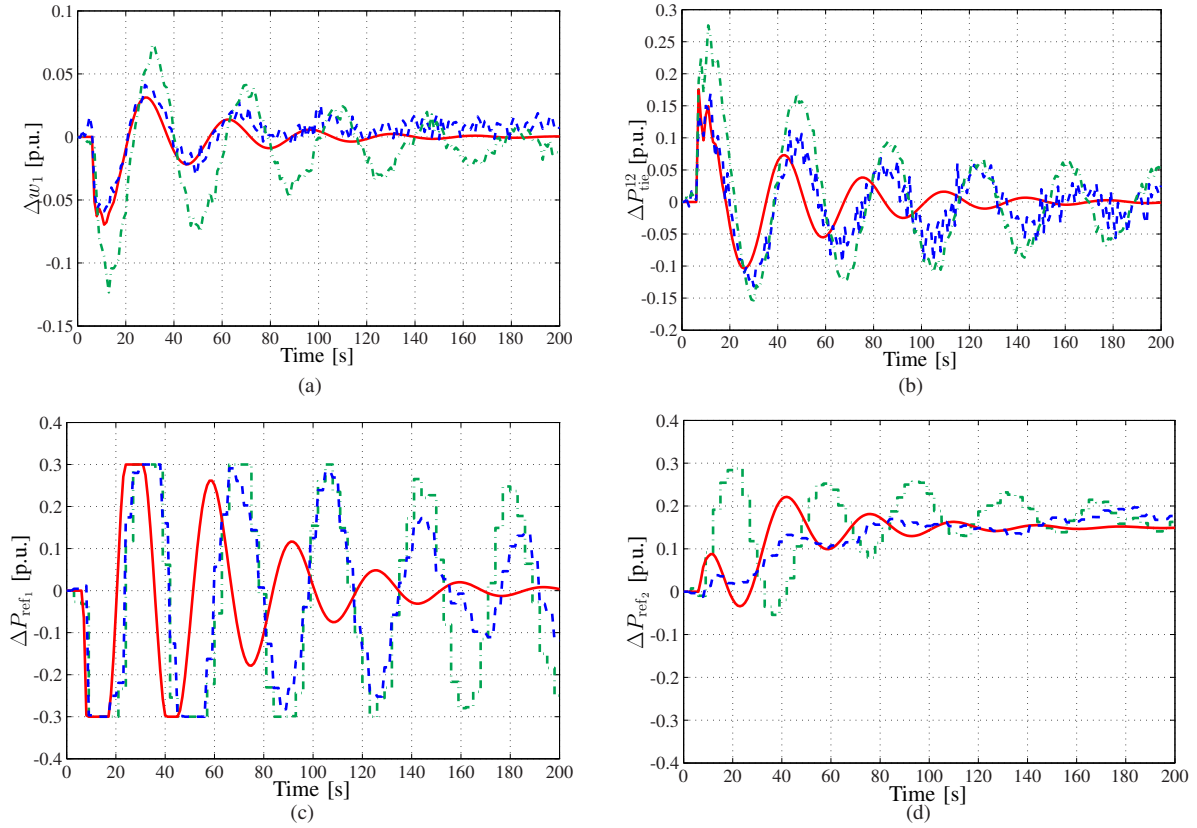


Fig. 5. Closed-loop responses of *synchronous* agents with *faster output / slower input* sampling rates using single-rate KF in red (solid); proposed distributed MPC with multi-rate KF in blue (dashed); distributed MPC with multi-rate decentralized KF in green (dash-dotted).

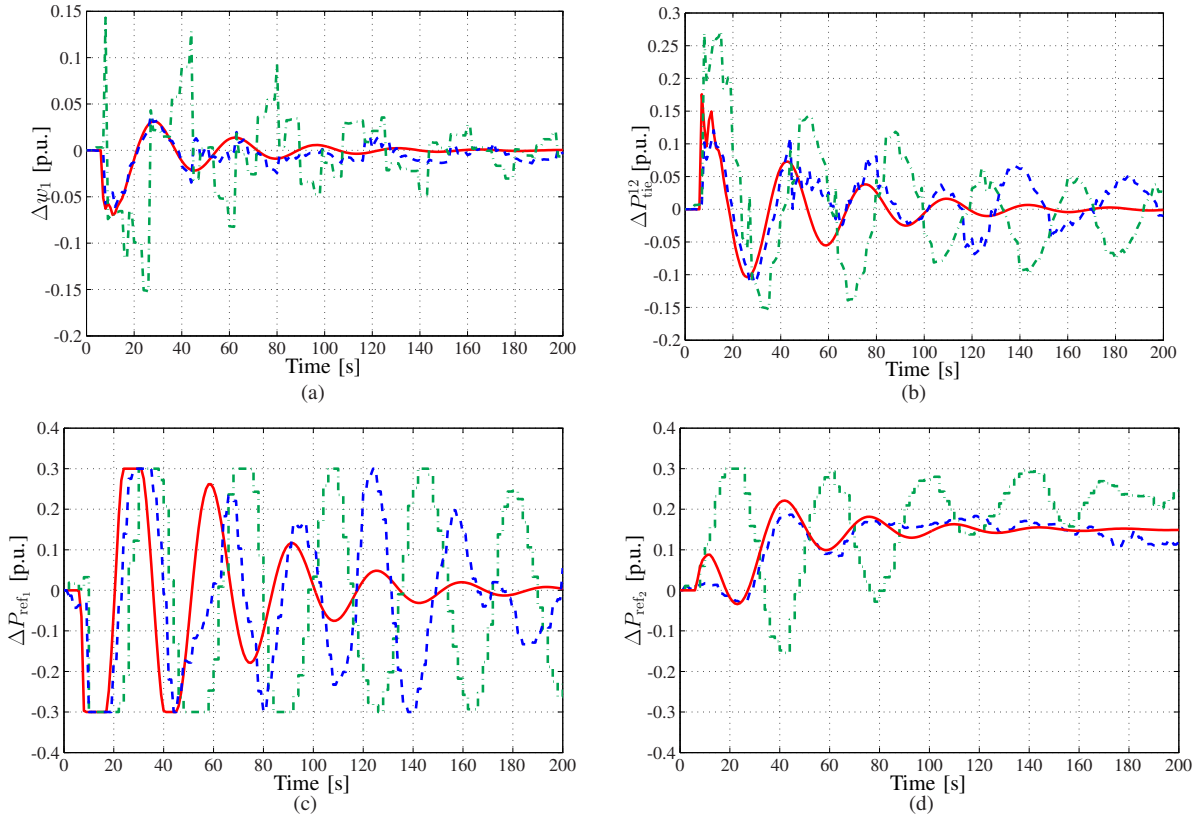


Fig. 6. Closed-loop responses of *asynchronous* agents with *slower output / faster input* sampling rates using single-rate KF in red (solid); proposed distributed MPC with multi-rate KF in blue (dashed); distributed MPC with multi-rate decentralized KF in green (dash-dotted).

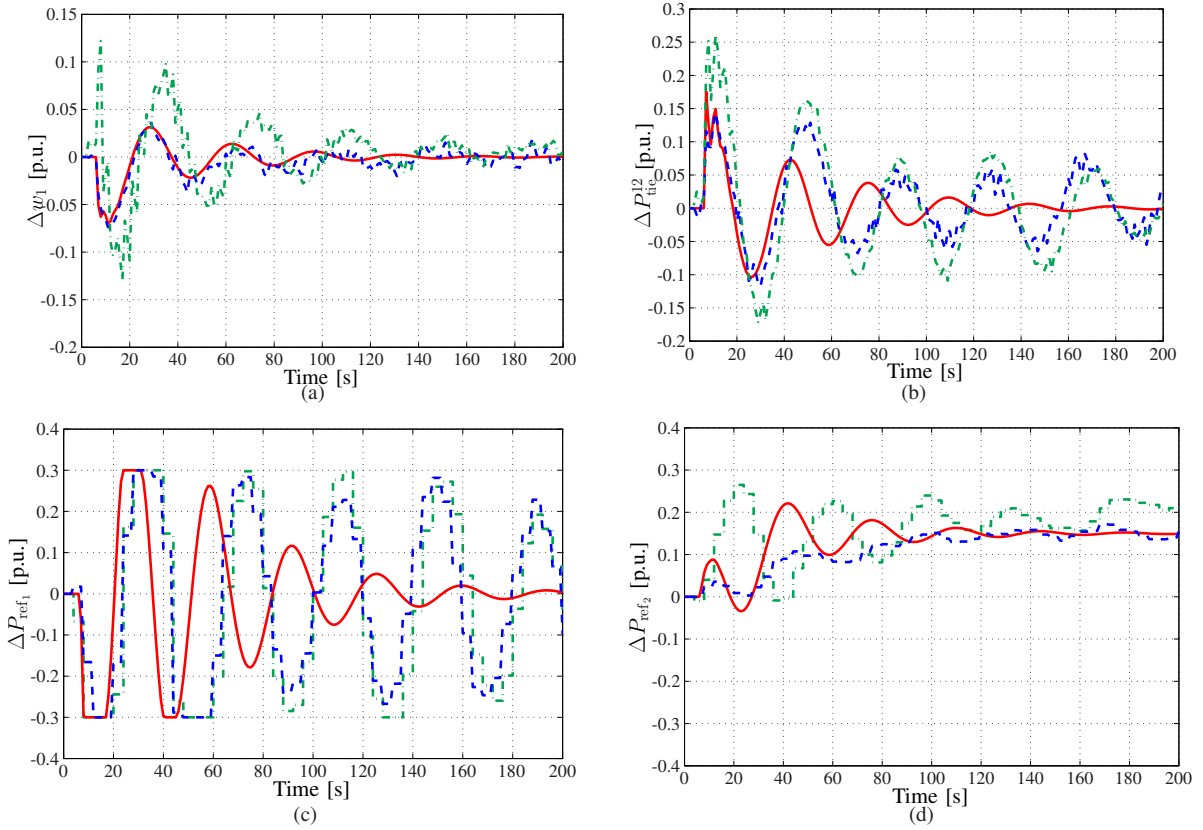


Fig. 7. Closed-loop responses of *asynchronous* agents with *faster output / slower input* sampling rates using single-rate KF in red (solid); proposed distributed MPC with multi-rate KF in blue (dashed); distributed MPC with multi-rate decentralized KF in green (dash-dotted).

ACKNOWLEDGMENTS

This research is supported by the Irish Programme for Research in Third Level Institutions (Cycle 4) (funded under the National Development Plan 2007-2013 with assistance from the European Regional Development Fund), and the VENI project “Intelligent multi-agent control for flexible co-ordination of transport hubs” (project 11210) of the Dutch Technology Foundation STW, a subdivision of the Netherlands Organization for Scientific Research (NWO).

REFERENCES

- [1] R. R. Negenborn, Z. Lukszo, and H. Hellendoorn, *Intelligent Infrastructures*. Springer, 2010.
- [2] R. R. Negenborn, B. De Schutter, and J. Hellendoorn, “Multi-agent model predictive control for transportation networks: Serial versus parallel schemes,” *Engineering Applications of Artificial Intelligence*, vol. 21, no. 3, pp. 353–366, April 2008.
- [3] R. Vadigepalli and F. J. Doyle, “A distributed state estimation and control algorithm for plantwide processes,” *IEEE Transactions on Control Systems Technology*, vol. 11, no. 1, pp. 119–127, 2003.
- [4] E. Camacho, F. Rubio, M. Berenguel, and L. Valenzuela, “A survey on control schemes for distributed solar collector fields. Part II: Advanced control approaches,” *Solar Energy Journal*, vol. 81, no. 1, pp. 1252–1272, February 2007.
- [5] T. Knudsen, T. Bak, and M. Soltani, “Distributed control of large-scale offshore wind farms,” in *Proc. European Wind Energy Conference and Exhibition*, Marseille, France, March 2009.
- [6] J. Yan and R. R. Bitmead, “Incorporating state estimation into model predictive control and its application to network traffic control,” *Automatica*, vol. 41, pp. 595–604, April 2005.
- [7] A. N. Venkat, I. A. Hiskens, J. B. Rawlings, and S. Wright, “Distributed MPC strategies with application to power system automatic generation control,” *IEEE Transactions on Control Systems Technology*, vol. 16, no. 6, pp. 1192–1206, November 2008.
- [8] W. Al-Gherwi, H. Budman, and A. Elkamel, “Selection of control structures for distributed model predictive control in the presence of model errors,” *Journal of Process Control*, vol. 20, no. 3, pp. 270–284, March 2010.
- [9] S. Li, Y. Zhang, and Q. Zhu, “Nash-optimization enhanced distributed model predictive control applied to the Shell benchmark problem,” *Information Sciences*, vol. 170, no. 2-4, pp. 329–349, February 2005.
- [10] M. Mercangoz and F. J. Doyle, “Distributed model predictive control of an experimental four-tank system,” *Journal of Process Control*, vol. 17, no. 3, pp. 297–308, March 2007.
- [11] R. Scattolini, “Architectures for distributed and hierarchical model predictive control - A review,” *Journal of Process Control*, vol. 19, no. 5, pp. 723–731, 2009.
- [12] T. Keviczky, F. Borrelli, K. Fregene, D. Godbole, and G. Balas, “Decentralized Receding Horizon Control and Coordination of Autonomous Vehicle Formations,” *IEEE Transactions on Control Systems Technology*, vol. 16, no. 1, pp. 19–33, January 2008.
- [13] K. Szabat and T. Orłowska-Kowalska, “Performance improvement of industrial drives with mechanical elasticity using nonlinear adaptive Kalman filter,” *IEEE Transactions on Industrial Electronics*, vol. 55, no. 3, pp. 1075–1084, March 2008.
- [14] Y. Soo-Suh, “Attitude Estimation by Multiple-Mode Kalman Filters,” *IEEE Transactions on Industrial Electronics*, vol. 53, no. 4, pp. 1386–1389, August 2006.
- [15] A. Giovanni-Beccuti, S. Mariéthoz, S. Cliquenois, S. Wang, and M. Morari, “Explicit model predictive control of DC-DC switched-mode power supplies with extended Kalman Filtering,” *IEEE Transactions on Industrial Electronics*, vol. 56, no. 6, pp. 1864–1874, June 2009.
- [16] J. M. Morris, “The Kalman Filter: a robust estimator for some classes of linear quadratic problems,” *IEEE Transactions on Information Theory*, vol. 22, no. 5, pp. 526–534, September 1976.
- [17] J. M. Torrealblanca, D. M. de la Peña Sequedo, and E. F. Camacho, “Distributed model predictive control based on a cooperative game,” *Optimal Control Applications & Methods*, vol. 32, no. 2, pp. 153–176, 2010.
- [18] S. Skogestad, M. Morari, and J. C. Doyle, “Robust control of ill-conditioned plants: high-purity distillation,” *IEEE Transactions on Automatic Control*, vol. 33, no. 12, pp. 1092–1105, December 1988.
- [19] K. Menighed and J. Yamé, “Distributed state estimation and model predictive control: Application to fault tolerant control,” in *Proc. IEEE International Conference on Control and Automation*, Christchurch, New Zealand, December 2009, pp. 936–941.
- [20] R. Scattolini and N. Schiavoni, “A multi-rate model based predictive control,” *IEEE Transactions on Automatic Control*, vol. 40, no. 6, pp. 1093–1097, June 1995.
- [21] M. Embiruçu and C. Fontes, “Multirate multivariable generalized predictive control and its application to a slurry reactor for ethylene polymerization,” *Chemical Engineering Science*, vol. 61, no. 17, pp. 5754–5767, September 2006.
- [22] R. S. Gopinath, B. W. Bequette, R. J. Roy, and H. Kaufman, “Multirate MPC design for a nonlinear drug infusion system,” in *Proc. American Control Conference*, Baltimore, Maryland, June-July 1994, pp. 102–106.
- [23] M. Ohshima, I. Hashimoto, H. Ohno, M. Takeda, T. Yoneyama, and F. Gotoh, “Multirate multivariable model predictive control and its application to a polymerization reactor,” *International Journal of Control*, vol. 59, no. 3, pp. 731–742, 1994.
- [24] P. Albertos and J. Salt, “Receding horizon control of non-uniformly sampled-data systems,” in *Proc. American Control Conference*, vol. 6, 1999, pp. 4300–4304.
- [25] P. Carini, R. Micheli, and R. Scattolini, “Multi-rate self-tuning predictive control with application to a binary distillation column,” *International Journal of Systems Science*, vol. 21, pp. 51–64, 1990.
- [26] J. Sheng, T. Chen, and S. L. Shah, “Generalized predictive control for non-uniformly sampled systems,” *Journal of Process Control*, vol. 12, pp. 875–885, 2002.
- [27] R. Scattolini, “Self-tuning control of systems with infrequent and delayed output sampling,” *Proc. IEE, Part D*, vol. 135, pp. 213–221, 1988.
- [28] M. Farina, G. Ferrari-Trecate, and R. Scattolini, “Moving horizon state estimation of large-scale constrained partitioned systems,” *Automatica*, vol. 46(5), pp. 910–918, 2010.
- [29] J. H. Lee, M. S. Gelormino, and M. Morari, “Model predictive control of multi-rate sampled-data systems: a state-space approach,” *International Journal of Control*, vol. 55, no. 1, pp. 153–191, January 1992.
- [30] J. M. Maciejowski, *Predictive Control with Constraints*. Prentice Hall, UK, 2002.
- [31] L. Giovanini and J. Balderud, “Game approach to distributed model predictive control,” in *Proc. International Control Conference*, Glasgow, UK, December 2006.
- [32] E. Camponogara, D. Jia, B. H. Krogh, and S. Talukdar, “Distributed Model Predictive Control,” *IEEE Control Systems Magazine*, pp. 44–52, February 2002.
- [33] D. Gu, “A Differential Game Approach to Formation Control,” *IEEE Transactions on Control Systems Technology*, vol. 16, no. 1, pp. 85–93, January 2008.
- [34] P. Kumar and J. V. Schuppen, “On Nash Equilibrium Solutions In Stochastic Dynamic Games,” *IEEE Transactions on Automatic Control*, vol. 25, no. 6, pp. 1146–1149, December 1980.
- [35] L. Wang, *Model Predictive Control System Design and Implementation Using MATLAB*. Springer, UK, 2009.
- [36] J. B. Rawlings and D. Q. Mayne, *Model Predictive Control: Theory and Design*. Nob Hill Publishing, LLC, 2009.